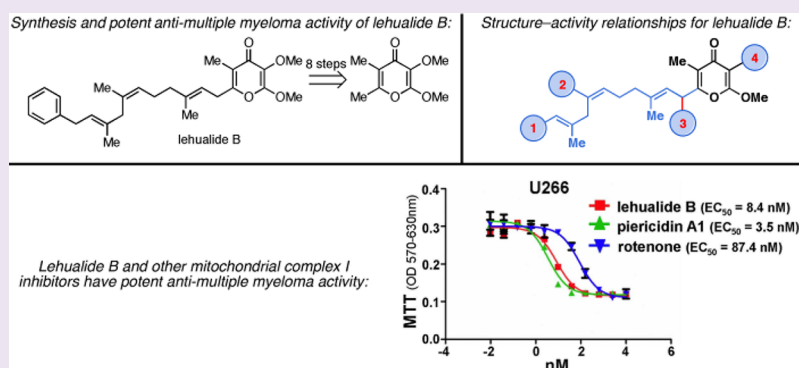


Synthesis and SAR of Lehualide B: A Marine-Derived Natural Product with Potent Anti-Multiple Myeloma Activity

Valer Jeso,[†] Chunying Yang,[‡] Michael D. Cameron,[#] John L. Cleveland,^{*,‡} and Glenn C. Micalizio^{*,†}

[†]Departments of Chemistry, [‡]Cancer Biology, and [#]Molecular Therapeutics, The Scripps Research Institute, Scripps Florida, Jupiter, Florida 33458, United States

Supporting Information



ABSTRACT: We report a concise and convergent laboratory synthesis of the rare marine natural product lehualide B that has led to the discovery that (1) this compound has low nanomolar activity against human multiple myeloma cells and (2) the anticancer effects of lehualide B and its analogues are selective (i.e., they are approximately 2–3 orders of magnitude less toxic to human breast cancer cells). Synthetic lehualide B is shown to be an effective inhibitor of complex I of the mitochondrial electron transport chain, with potency similar to that observed for the terrestrial natural products piericidin A1 and rotenone, an observation that led to the discovery that piericidin A1 is also selectively cytotoxic toward human multiple myeloma cells. Interestingly, synthetic derivatives of lehualide B that resemble verticipyron (an established complex I inhibitor composed of a γ -pyrone and a simple monounsaturated hydrophobic chain) lack the potent antimyeloma activity of the natural product. Finally, the synthesis and evaluation of a collection of lehualide-inspired analogues led to the elucidation of structure–activity relationships for this rare natural product that established important roles for the substituted γ -pyrone headgroup and the skipped polyene side chain.

Marine-derived natural products continue to provide an exciting collection of therapeutically valuable leads that, because of their usually low availability from natural sources, require chemical synthesis to drive efforts focused on evaluating their potential value as medicines.^{1–3} The lehualides (Figure 1A) are a family of pyrone-containing natural products recently isolated from Hawaiian and Tongan marine sponges (*Plakortis* sp.) that were originally shown to possess modest anticancer properties against ovarian (IGROV-ET) and leukemia (K562) cell lines.^{4,5} Notably, members of this class have disparate toxicity profiles that stem from subtle variations in pyrone substitution and the composition of their aliphatic tail. For example, lehualides A–D (1–4) show varying brine shrimp toxicity that suggests that the γ -pyrone motif imparts maximal toxicity.⁴ Further, lehualides A (1) and C (3) do not display toxicity in ovarian or leukemia cell lines that are sensitive to lehualides B (2) and D (4) [2, GI₅₀ = 830 nM (IGROV-ET); 4, GI₅₀ = 730 nM (IGROV-ET) or 230 nM (K562)]. In line with these observations that indicate a role for the γ -pyrone in imparting maximal toxicity, the most recently isolated lehualides (F–I; 6–9) that contain α -pyrones similar to

lehualide A (1) and monounsaturated or saturated hydrophobic side chains are much less toxic (1–2 orders of magnitude) than lehualides B and D.⁵

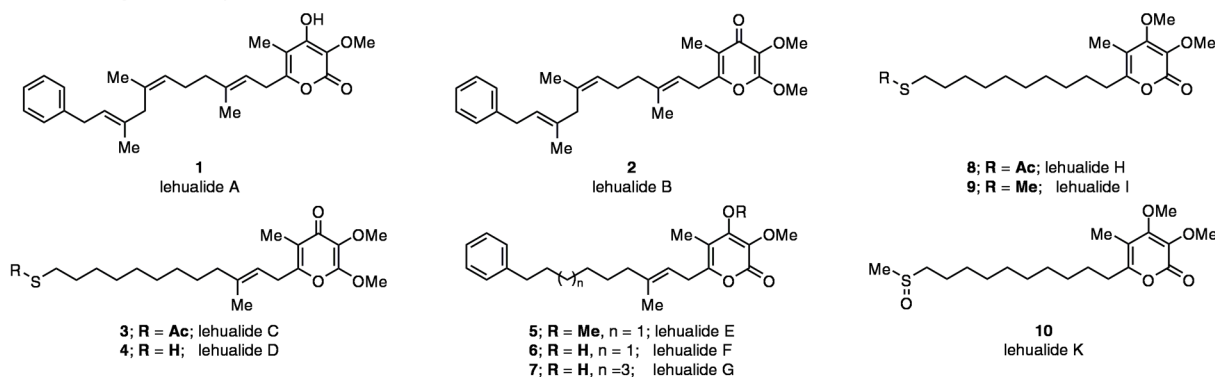
While the mechanism of action for the most toxic lehualides has heretofore not been elucidated, their common pyrone structure is reminiscent of the pyridine core of piericidin A1 and the quinone of ubiquinone (Figure 1B). Related γ -pyrone moieties are found in several other cytotoxic natural products (Figure 1C)^{6–25} that have a wide variety of activities as insecticidal, anticancer, antifungal, antibacterial and immunosuppressive agents.^{6–25} Some of these compounds have been shown to block the voltage-gated potassium channel Kv1.3 and to potently inhibit the mitochondrial electron transport chain protein NADH-ubiquinone reductase (complex I), with IC₅₀'s as low as 0.3 nM (verticipyron analogues).²⁶ Finally, germane to our studies, a subset of potent complex I inhibitors have

Received: October 26, 2012

Accepted: March 18, 2013

Published: April 2, 2013

A. The lehualide family of natural products.



B. Relationship of cytotoxic lehualides to piericidin A1 and ubiquinone.

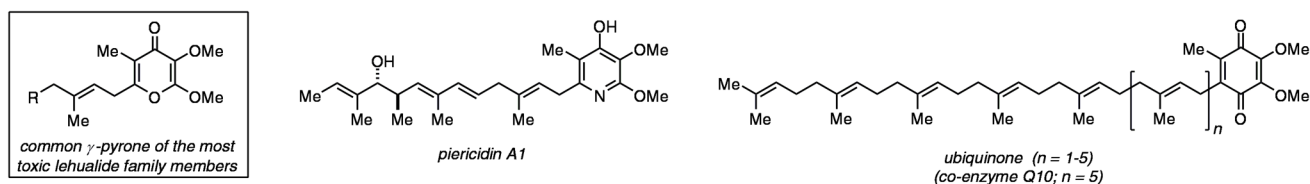
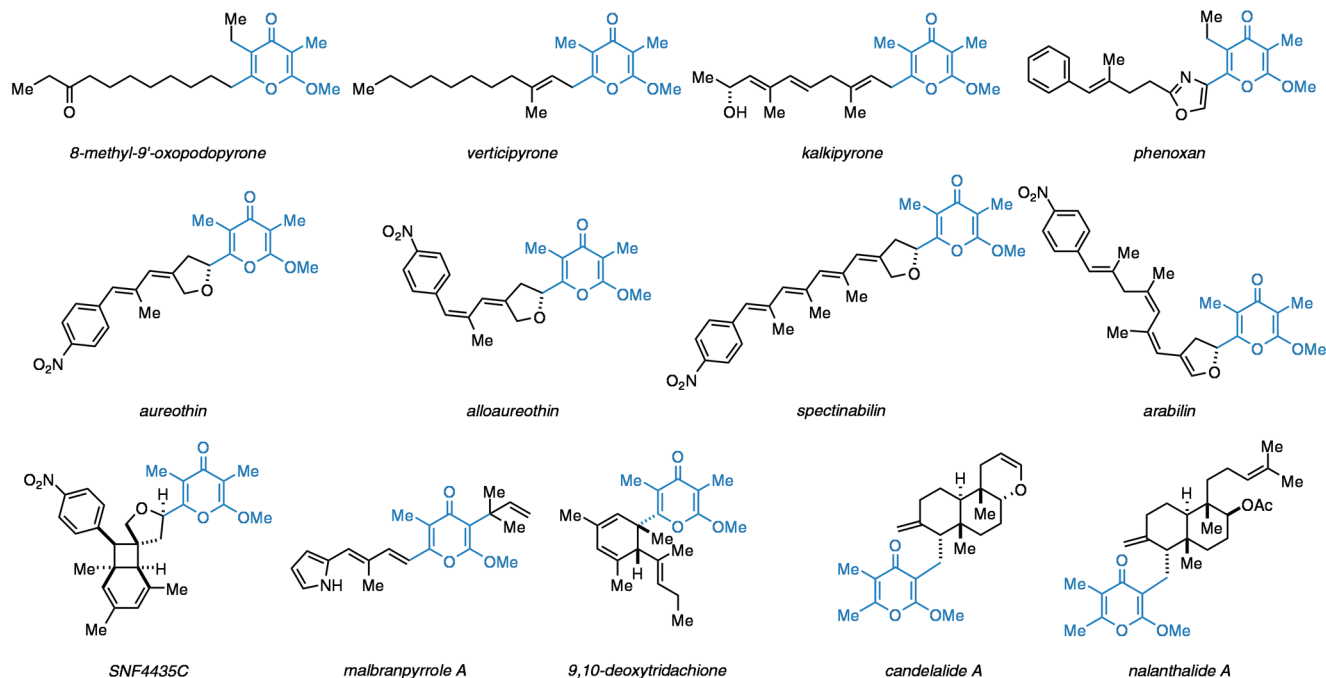
C. A selection of γ -pyrone-containing natural products.

Figure 1. Introduction to the lehualides and related natural products.

received attention as selective antitumor agents, yet the mechanism responsible for this activity has not been resolved.^{27,28}

Recent studies by Boger and colleagues focused on understanding the activity of piericidin A1 revealed that complex I inhibition is necessary but not sufficient to confer potent cytotoxicity to synthetic analogues. Hypotheses stated to explain this included a potential differential ability to access the cellular target, subtle distinctions between multiple binding sites on complex I, and/or a role for additional (undefined) biological targets.²⁸

The most potent members of the lehualide family are structurally related to the natural products depicted in Figure 1B and C, yet they have unique features that include a 2,3-

dimethoxy-substituted γ -pyrone and a hydrophobic tail that contains three trisubstituted alkenes that are uniformly "skipped" (nonconjugated) with respect to neighboring π -systems (i.e., 2). While not possessing a single chiral center, the stereochemistry and substitution of this skipped-polyunsaturated tail renders lehualide B a significant challenge to modern synthetic organic chemistry.²⁹

The structural similarity of lehualide B to natural products known to possess an array of medically relevant biological activities, and the lack of a robust supply from natural sources prompted us to define a concise synthetic entry to this natural product that would allow assessment of the medicinal value of this target. In pursuit of these goals, our efforts have led to (1) the total synthesis of lehualide B and 25 synthetic analogues;

(2) the discovery that lehualide B is selectively cytotoxic to multiple myeloma cells at low nanomolar concentrations; (3) the observation that lehualide B, and closely related synthetic analogues, totally abolish long-term growth of chemoresistant multiple myeloma cells; and (4) the discovery that lehualide B is a potent inhibitor of mitochondrial complex I.

RESULTS AND DISCUSSION

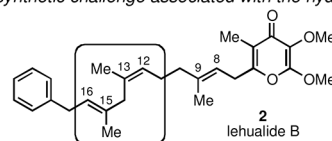
Total Synthesis of Lehualide B. Given anticipated difficulties associated with synthesizing the skipped polyene tail of **2**, our retrosynthetic strategy was primarily influenced by the most challenging structural motif in this region: the C12–C16 1,4-diene that houses both an (*E*)- and (*Z*)-trisubstituted alkene (Figure 2A). While modern carbonyl olefination or metal-catalyzed cross-coupling are commonly used for the synthesis of trisubstituted alkenes, neither of these is optimal for the challenge associated with this section of lehualide B. Specifically, methods based on carbonyl olefination are plagued by challenges associated with the control of stereochemistry in establishing the trisubstituted alkenes and with difficulties associated with advancing β,γ -unsaturated systems.³⁰ Metal-catalyzed cross-coupling is similarly complex because of the multistep nature of synthetic pathways to generate the stereodefined coupling partners (Figure 2B) and associated problems with regio- and stereocontrol in the reaction of intermediate π -allyl complexes.³¹ Given these hurdles we sought an alternative method for preparing this stereodefined subunit.

We recently established a reductive cross-coupling process that proceeds by stereoselective union of allylic alcohols with alkynes and that generates two stereodefined trisubstituted alkenes along with a central C–C bond.³² In analyzing the lehualide B structure this reaction seemed ideal for establishing the C14–C15 bond with concomitant generation of each stereodefined trisubstituted alkene of the 1,4-diene: a bond construction that would ensue with stereoundefined and “unactivated” π -systems (Figure 2C).

Using this bond construction as a central feature of our design, the retrosynthetic strategy to lehualide B that emerged was comprised of a simple sequence that embraced the utility of allylic alcohols for establishing all of the trisubstituted alkenes in this target (Figure 2D). Well-established Claisen rearrangement chemistry^{33,34} was envisioned as a means to convert allylic alcohol **12** to an (*E*)-trisubstituted alkene (as in **11**), while Ti-mediated, alkoxide-directed reductive cross-coupling could then be employed to convert allylic alcohol **11** to the desired (*Z*)-trisubstituted C12–C13 alkene of lehualide B. In this latter process, stereochemical control was predicted in accord with our previous studies that put forth an empirical model based on a boat-like transition state geometry for carbometalation that features minimization of A1,2-strain (Figure 2C; A \rightarrow B \rightarrow C).³²

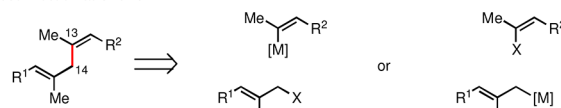
With this retrosynthetic strategy in mind, we began with synthesis of the requisite 2,3-dimethoxy-5,6-dimethyl γ -pyrone **13**. As shown in Scheme 1A, iodosobenzene diacetate-mediated oxidation of β -ketoester **14** in methanol provided the α -methoxy- β -ketoester **15** in 70% yield.³⁵ Deprotonation with LDA (2.2 equiv), followed by addition of Weinreb amide **16**, then delivered the tricarbonyl **17** as a mixture of isomers. Stirring this tricarbonyl in neat H₂SO₄ (for 21 h) then generated the γ -pyrone **13** in 24% yield over the two-step sequence.³⁶

A. Lehualide B - synthetic challenge associated with the hydrophobic tail.

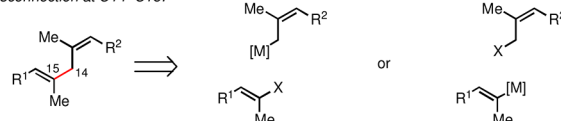


B. Strategic analysis for use of established convergent coupling chemistry.

• disconnection at C13–C14:

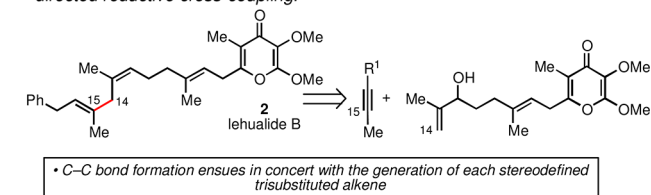


• disconnection at C14–C15:

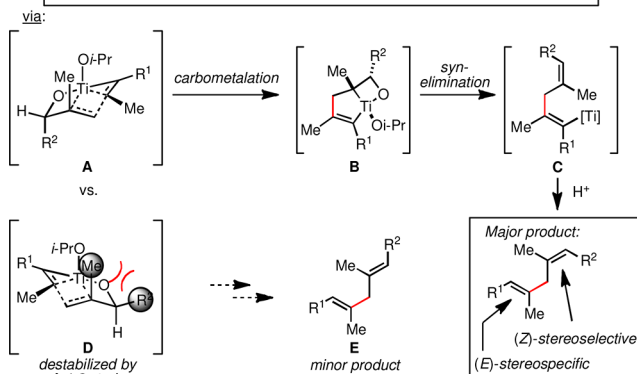


Both strategies require multi-step generation of each stereodefined coupling partner.

C. Addressing the C12–C16 1,4-diene of lehualide B by Ti-mediated alkoxide-directed reductive cross-coupling.



• C–C bond formation ensues in concert with the generation of each stereodefined trisubstituted alkene



D. A simple retrosynthetic analysis for lehualide B.

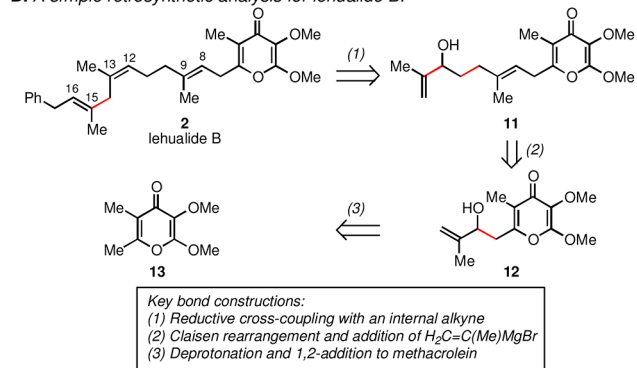
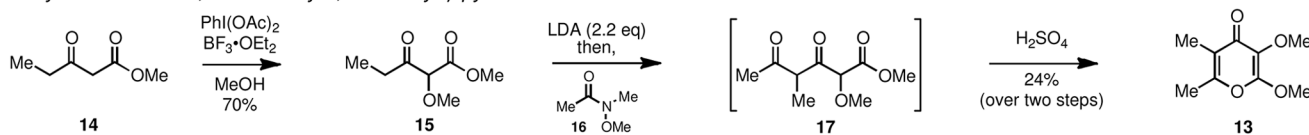


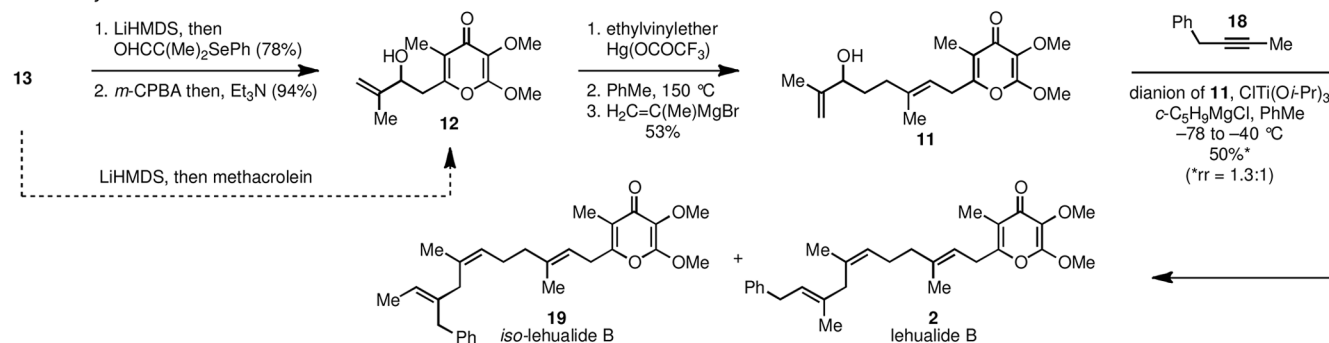
Figure 2. Development of a concise synthesis strategy for lehualide B.

Next, attempted addition of the extended enolate of **13** to methacrolein was problematic, likely because of competitive 1,4-addition (Scheme 1B). To avoid this issue, α -(phenylseleno)-isobutyraldehyde was used as the electrophile in reaction with the anion of **13**. Subsequent oxidation to the selenoxide was followed by *syn*-elimination *in situ* to deliver the desired allylic alcohol **12** in 73% yield (over two steps).³⁷ Next, Johnson orthoester Claisen rearrangement delivered the

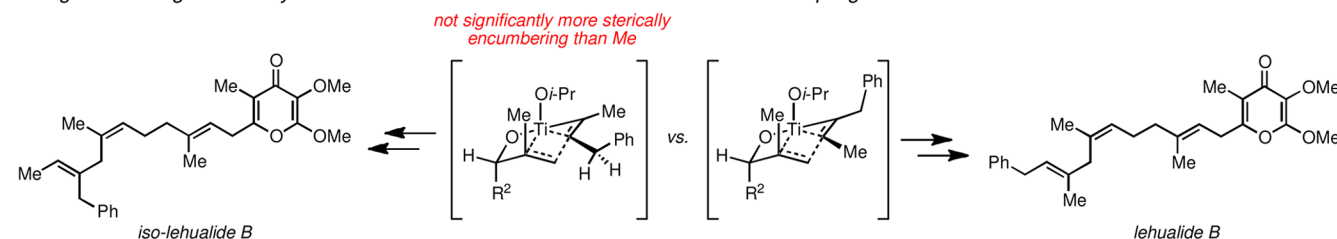
Scheme 1. Synthesis of Lehualide B

A. Synthesis of the 2,3-dimethoxy-5,6-dimethyl- γ -pyrone.

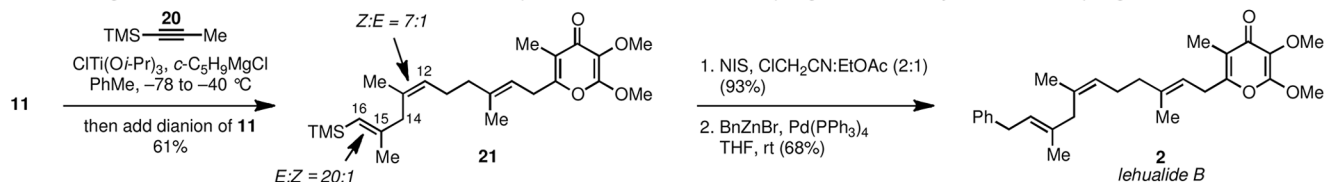
B. Total synthesis of lehualide B.



C. Origin of low regioselectivity in the Ti-mediated alkoxide-directed reductive cross-coupling.



D. Second-generation route to lehualide B based on sequential reductive cross-coupling and Pd-catalyzed cross-coupling.



desired γ,δ -unsaturated aldehyde (*E*:*Z* = 10:1),³⁸ which was then used to generate the functionalized allylic alcohol 11 by the addition of 2-propenylmagnesium bromide (53% yield over two steps).

Having the allylic alcohol 11 in hand, alkoxide-directed Ti-mediated reductive cross-coupling with 1-phenyl-2-butyne was then performed using slightly modified reaction conditions than previously reported for this stereoselective coupling process.³² Initial formation of a dianion of 11 (to mask the potential electrophilic character of the pyrone carbonyl) was followed by exposure to a preformed Ti-alkyne complex that was generated by treating 1-phenyl-2-butyne with a combination of $\text{CITi}(\text{O}i\text{-Pr})_3$ (6 equiv) and *c*- $\text{C}_5\text{H}_9\text{MgCl}$ (12 equiv). Warming from -78 to 0 °C, followed by an aqueous quench, delivered the coupled products in 50% combined yield.

Despite the success of this coupling process and the concise synthetic sequence (six steps from the simple γ -pyrone), the natural product was formed as an inseparable 1.3:1 mixture of regioisomers (2 and 19), where the minor product was derived from C–C bond formation occurring α - to the Bn substituent of the alkyne to deliver isolehualide B. This low selectivity was expected, as regiochemical control in functionalizing Ti-alkyne complexes typically requires substantial steric or electronic differentiation of the alkyne termini.³⁹ In the competing

transition states for carbometalation depicted in Scheme 1C, it is evident that the steric impediment of the Ph group can easily be avoided by simple bond rotation (this similar steric profile of Me and Bn is evident in their A values: Me = 1.7 kcal/mol; Bn = 1.8 kcal/mol⁴⁰).

To circumvent this problem, a straightforward solution was adopted that exploited the well-appreciated regioselectivity associated with Ti-mediated reductive cross-coupling reactions of TMS-substituted alkynes.³⁹ Specifically, metallacycle-mediated reductive cross-coupling of allylic alcohol 11 with TMS-alkene-containing 1,4-diene product 21 in 61% yield (*Z*:*E* = 7:1; *rs* \geq 20:1). Subsequent conversion to the vinyl iodide [NIS, $\text{ClCH}_2\text{CN}:\text{EtOAc}$ (2:1)],⁴¹ followed by Pd-catalyzed cross-coupling with benzylzinc bromide generated lehualide B in 64% yield over the final two-step sequence.⁴²

Anticancer Properties of Lehualide B. The concise synthesis of lehualide B fueled efforts to prepare sufficient quantities of the natural product to evaluate its anticancer properties. Our initial assessment of the effects of 0.1–10 μM doses of lehualide B on a cast of tumor cell lines was performed with MTT assays using estrogen receptor-positive (ER+) (MCF7, T47D) and triple negative (MDA-MB-231, HS578) breast cancer cells, and three multiple myeloma (MM) cell lines

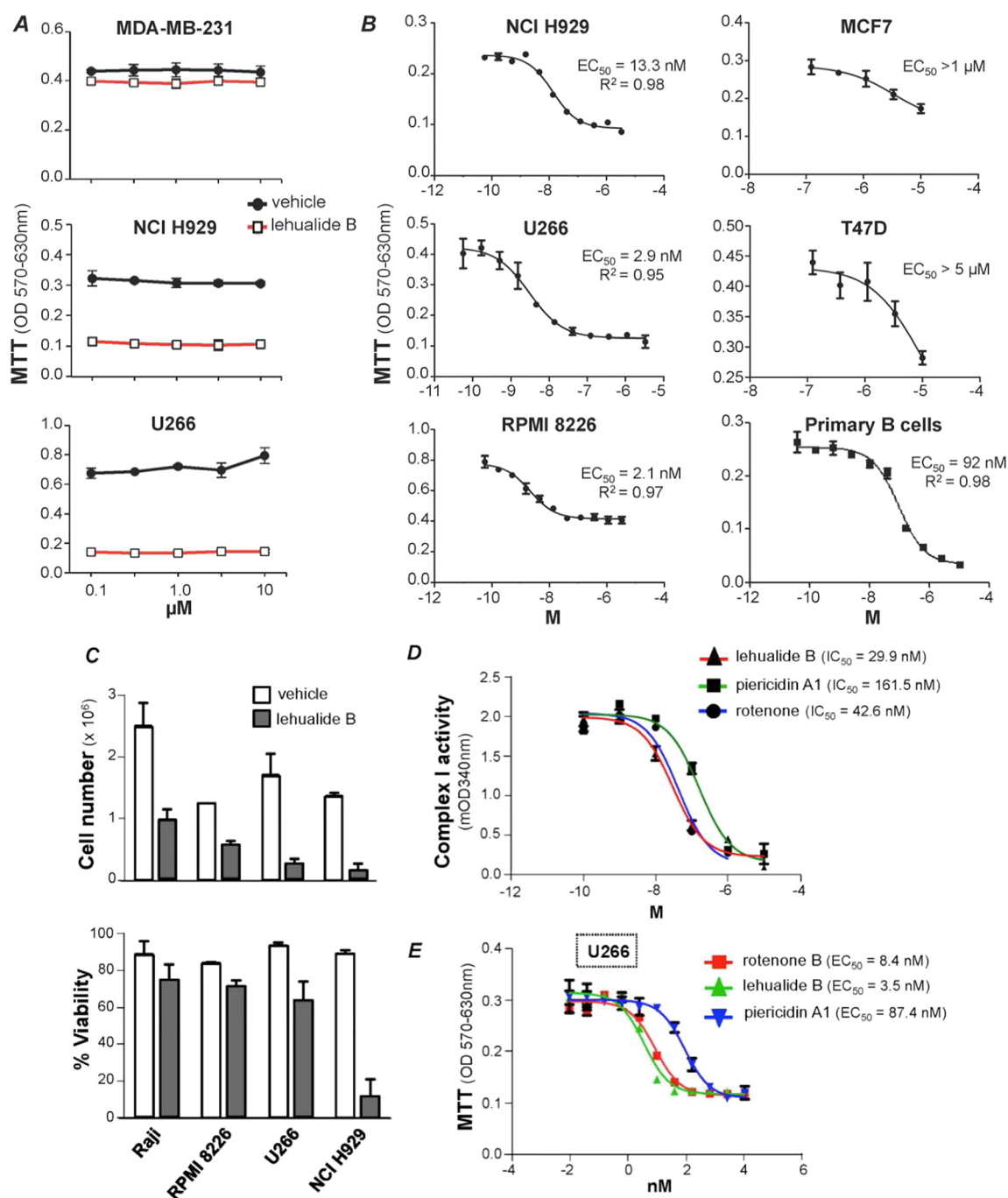


Figure 3. Lehualide B has potent and selective activity against multiple myeloma (MM) cells, impairs MM cell growth and survival, and is a potent inhibitor of complex I of the mitochondrial electron transport chain. (A) MTT assays were performed on MDA-MB-231 triple-negative breast cancer cells and on NCI H929 and U266 MM cells, which were treated with the indicated doses of lehualide B (3 days of culture). (B) The EC₅₀ values of lehualide B for the indicated MM cells (left) and bone marrow-derived primary mouse B cells were determined using 11-point dose–response MTT assays. For the ER+ breast cancer cells MCF7 and T47 D (right) the EC₅₀ was >1 μM (five-point dose–response MTT assays). Error bars are the SD of the mean ($n = 3$). (C) The indicated tumor cell lines were incubated with 1 μM lehualide B or vehicle. Cell numbers (top) and viability (bottom) were determined after 4 days ± lehualide B (30 nM). Error bars are the SD of the mean ($n = 2$). (D) Lehualide B blocks complex I. Mitochondrial complex I activity was measured using the MitoTox Complex I OXPHOS Activity assay kit. Error bars are the SD of the mean ($n = 4$). (E) Mitochondrial complex I inhibitors have potent anti-MM activity. U266 MM cells were treated with the indicated doses of lehualide B, piericidin A1, or rotenone for 3 days, and MTT assays were performed. Error bars are the SD of the mean ($n = 3$).

(NCI H929, U266, and RPMI-8226).⁴³ While there were essentially no effects of lehualide B on the growth of triple-negative breast cancer, and only modest effects on ER+ breast cancer cells, there were profound effects on multiple myeloma cells (Figure 3A). Indeed, MTT assays established very potent activity for lehualide B in all MM tumor cell lines investigated,

with EC₅₀ values of 2.1, 2.9, and 13 nM for RPMI-8226, U266 and NCI H929 MM cells, respectively. Interestingly, lehualide B was 3 orders of magnitude less effective vs MCF7 and T47D ER+ breast cancer cells (>1 μM, Figure 3) and >1 order of magnitude less toxic to mouse bone marrow-derived primary B cells cultured on stroma and in IL7 medium (EC₅₀ of 92 nM,

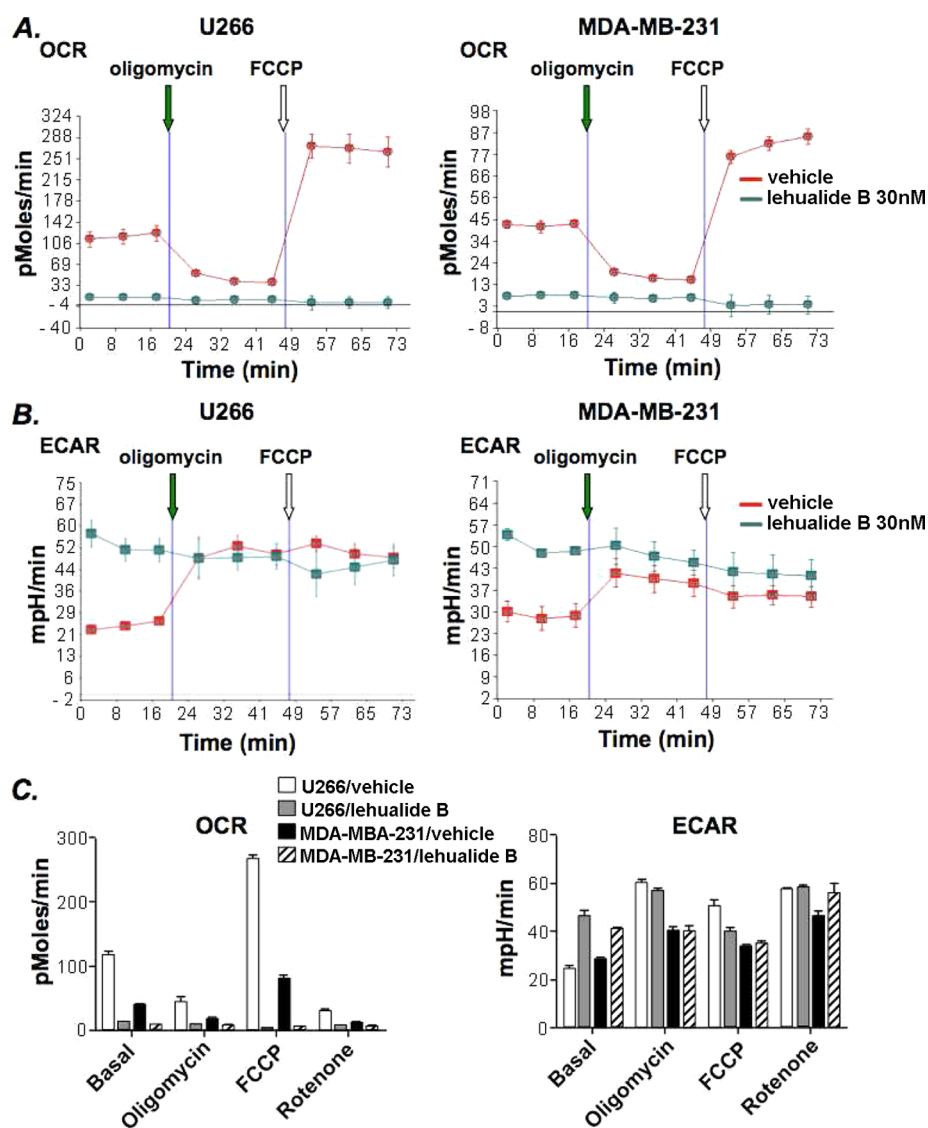


Figure 4. Lehualide B abolishes OXPHOS in multiple myeloma cells. (A,B) U266 (left panels) and MDA-MB-231 cells (right panels) (in 96 wells) were treated with vehicle (orange line) or with lehualide B (30 nM, teal line) for 1 h and then assessed for OCR (A) or ECAR (B) using the Seahorse Bioscience XF96 analyzer.⁴⁵ Measurements were determined every 7 min for six replicates, and error bars are standard error of the mean. After basal measurements cells were treated with the ATP synthase inhibitor oligomycin (green arrow), which induces increases in glycolysis (i.e., ECAR), followed by treatment with the mitochondrial uncoupling agent FCCP (white arrow), which measures mitochondrial respiratory reserves. Results shown are representative of four independent experiments. Note that lehualide B abolishes OCR and mitochondrial respiratory capacity. (C) Summary of OCR (left) and ECAR (right) analyses of U266 MM and MDA-MB-231 breast cancer cells. Note that the basal rates of OCR are ~3-fold higher in U266 MM cells than in MDA-MB-231 cells. Rotenone treatment allows measurement of mitochondrial-independent oxygen consumption, which was minimal in both tumor cell lines. Mean values were calculated before (basal) or after oligomycin, FCCP or rotenone treatment.

Figure 3B). Thus, there is significant selectivity associated with the cytotoxic profile of lehualide B.

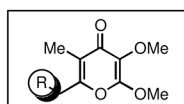
To address the mechanism by which lehualide B compromised MM cells, its effects were assessed on cell growth using standard growth assays and upon cell survival by trypan blue dye exclusion.⁴⁴ Human MM cells and Raji B lymphoma were plated in culture and then treated with lehualide B for two days. Notably, treatment with the natural product led to rapid and marked reductions in cell number that were accompanied by a loss in cell viability (Figure 3C) and cell shrinkage (especially in NCI H929 MM) typical of apoptotic cell death.

Given the structural similarity of the γ -pyrone group of lehualide B with the quinone of ubiquinone and the heterocycle

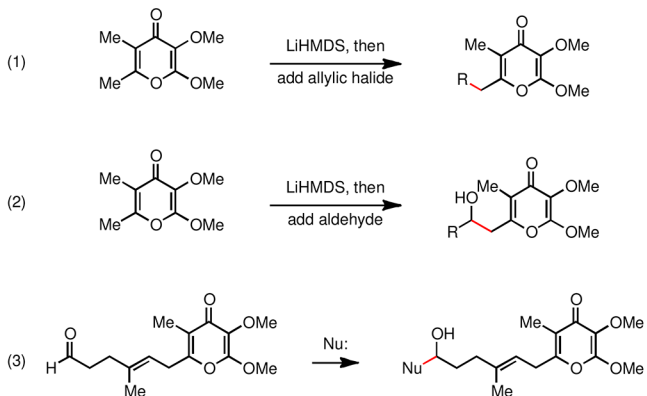
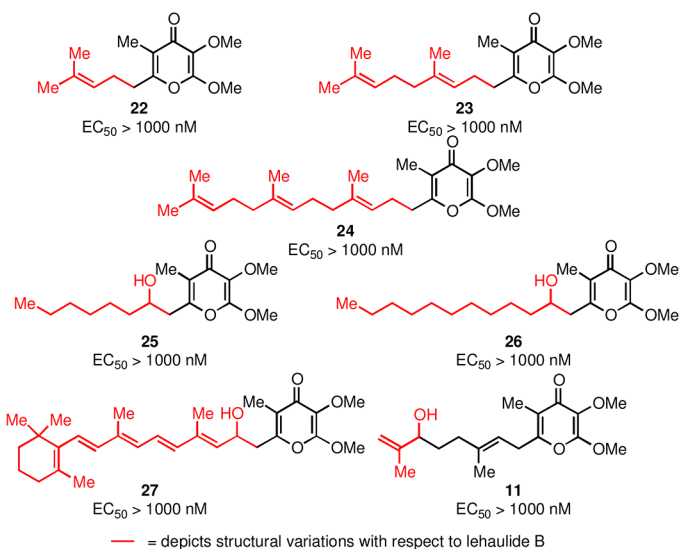
of piericidin A1, we tested if lehualide B was an inhibitor of complex I of the mitochondrial electron transport chain. Indeed, *in vitro* assays established that, like piericidin A1, lehualide B is a potent complex I inhibitor ($IC_{50} = 30$ nM; Figure 3D).

These findings suggested that other complex I inhibitors may display similar antimyeloma activity. Indeed, piericidin A1 and rotenone also block the proliferation of U266 and RPMI-8226 MM cells (Figure 3E and data not shown). Related to the profile of lehualide B, these agents were similarly ineffective vs breast cancer cells (data not shown). Thus, mitochondrial complex I inhibitors such as lehualide B and piericidin A1 are selective anticancer agents and have high potency against multiple myeloma. In addition to discovering this interesting

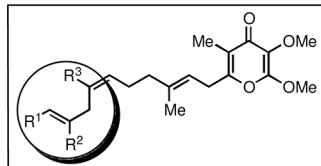
A. Role of the entire hydrophobic tail in defining anti-MM properties.



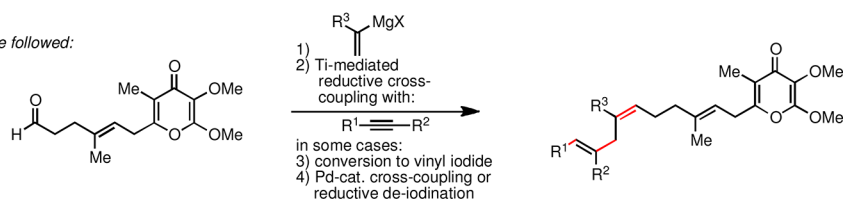
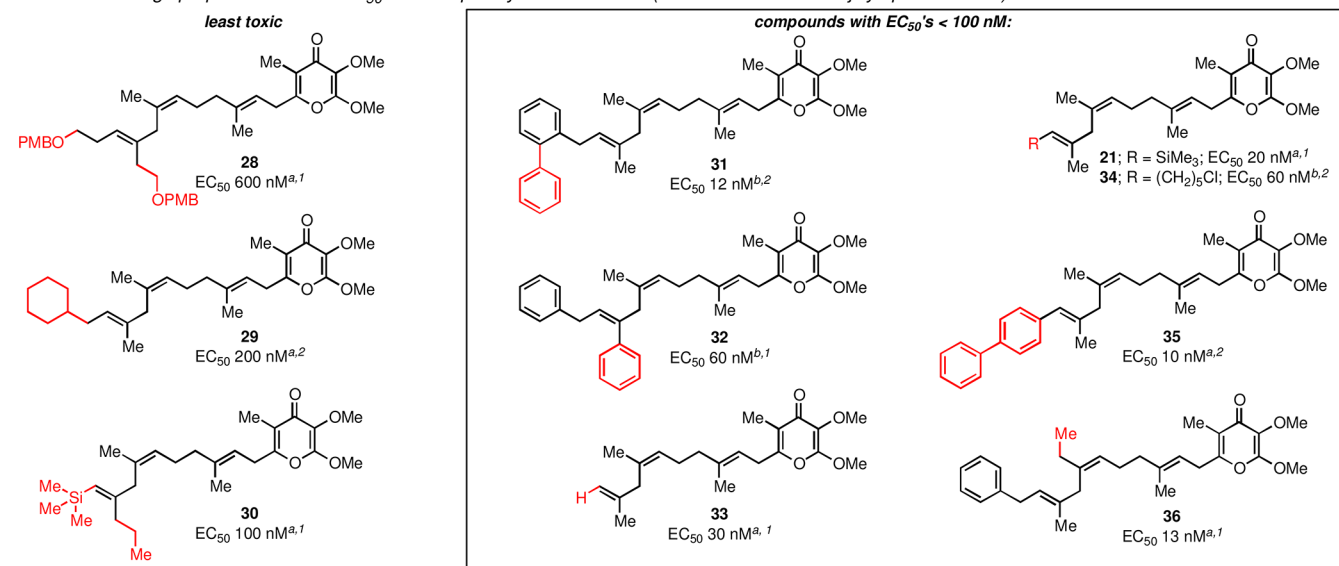
General chemical route to series I analogs:

B. EC_{50} 's of series I analogs vs. multiple myeloma (U266 cell line):

C. Role of the tail terminus in defining anti-MM properties.



General chemical route followed:

D. Series II analogs prepared and their EC_{50} 's in multiple myeloma cell lines (RPMI-8226/human Raji lymphoma/U266): 12 - 600 nM.a = a five-point dose-response curve was employed to determine these approximate EC_{50} values.b = an eleven-point dose-response curve was employed to determine EC_{50} values.

1 = evaluated in U266 cells.

2 = evaluated in human Raji lymphoma cells.

— = depicts structural variations with respect to lehalide B

Figure 5. Synthesis and evaluation of Series I analogs of lehalide B: Significance of the hydrophobic region.

anticancer activity of lehalide B, to our knowledge this is the first report that describes the potent and selective anti-MM properties associated with pteridin A1.

To assess why MM cells are so sensitive to complex I inhibitors such as lehalide B while others such MDA-MB-231 breast cancer cells are not, we evaluated the metabolic status of these tumor cells and how this is affected by treatment with lehalide B using the Seahorse Bioscience XF96 Analyzer.⁴⁵

Specifically, we assessed the effects of lehalide B on the oxygen consumption rate (OCR, a measure of oxidative phosphorylation [OXPHOS]) and extracellular acidification rate (ECAR, a measure of aerobic glycolysis). Notably, these analyses demonstrated that U266 MM cells have much higher rates of OCR than MDA-MB-231 breast cancer cells and that lehalide B treatment abolishes OCR and depletes mitochondrial energy reserves, as demonstrated by treatment of cells with the

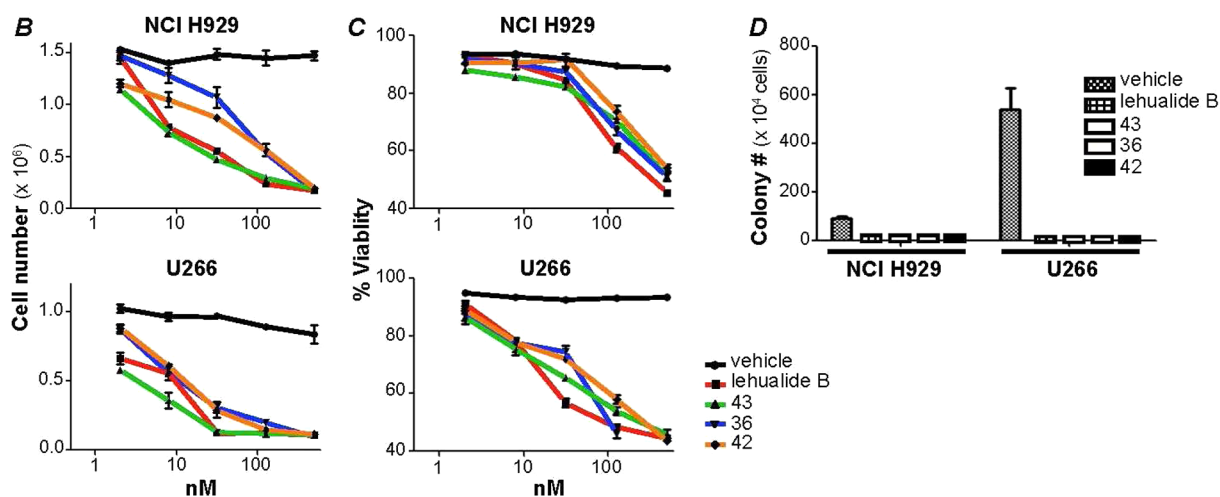
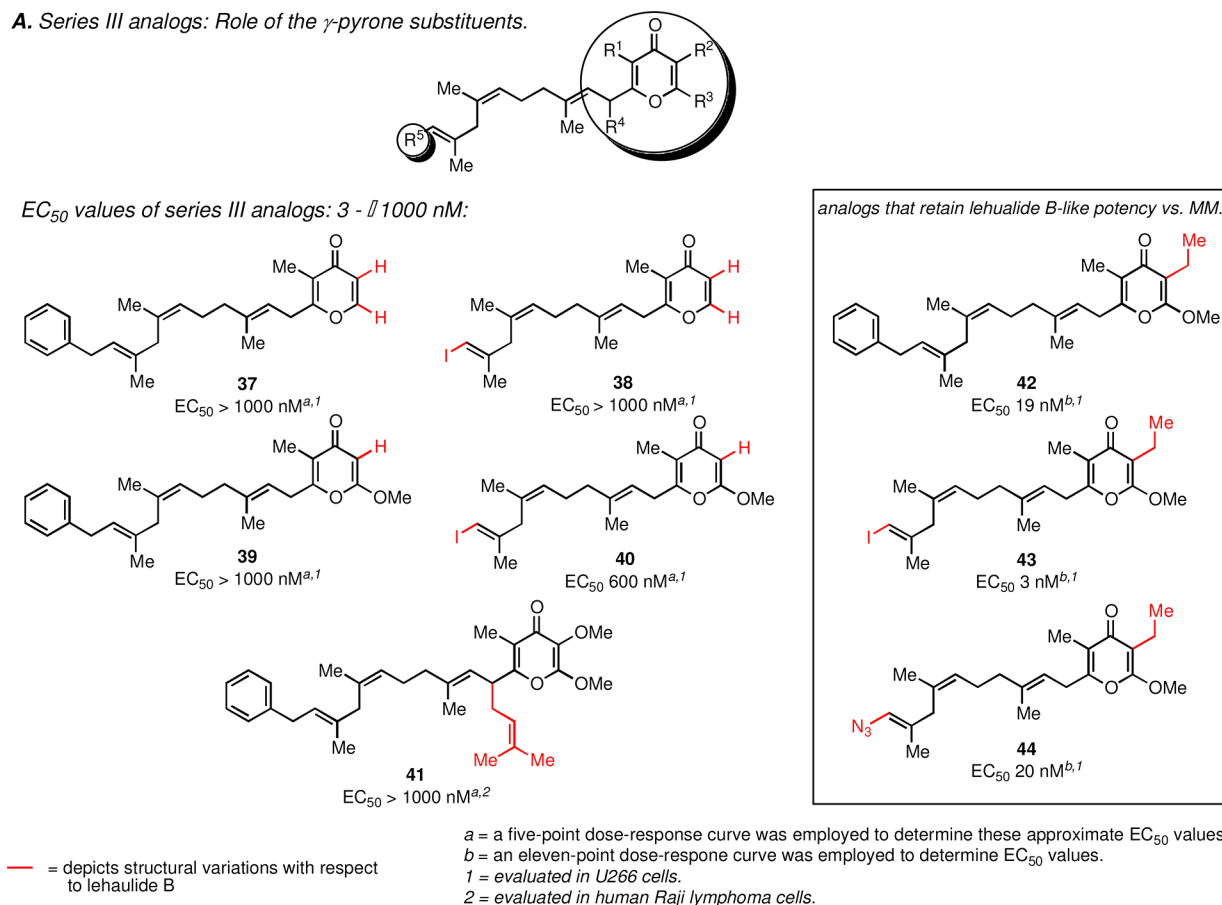
A. Series III analogs: Role of the γ -pyrone substituents.

Figure 6. (A) Synthesis and evaluation of Series III analogues of lehualide B: Significance of substitution about the γ -pyrone hydrophilic head. Lehualide B and key analogues compromise growth and survival of multiple myeloma. (B,C) NCI H929 and U266 cells were cultured for 3 days with vehicle or the indicated doses of lehualide B or key analogues and cell number (B) and percent viable cells (i.e., those excluding trypan blue) (C) were determined by counting with a hemocytometer. (D) The indicated MM cells were plated in methylcellulose containing the indicated agents (500 nM). Colony numbers were determined on day 10. Error bars are the SD.

mitochondrial uncoupling agent FCCP (Figure 4). Furthermore, lehualide B causes a marked shift in metabolism to ECAR (Figure 4B,C). We conclude that U266 MM cells rely on OXPHOS (OCR) to support their metabolism, which is disabled by lehualide B, whereas the metabolism of MDA-MB-231 breast cancer cells rather relies on aerobic glycolysis.

Synthesis and Activity of Lehualide B Analogues. The potent and selective anti-MM profile of lehualide B, and the

lack of substantive structure–activity relationships for this rare marine-derived natural product, prompted analyses of the molecular features essential for its antimyeloma activity. We investigated the role that three key regions of the natural product play in imparting anti-MM properties: (1) the aromatic tail, (2) the hydrophobic linker, and (3) the γ -pyrone hydrophilic headgroup.

Series I analogues were prepared to evaluate the significance of the entire hydrophobic tail of lehualide B (including the aromatic terminus). These analogues were generated as described in Figure 5A and follow either (1) nucleophilic addition of a pyrone-derived anion to an allylic halide (eq 1); (2) nucleophilic addition of a pyrone-derived anion to an aldehyde (eq 2); or (3) nucleophilic addition to a pyrone-containing unsaturated aldehyde (eq 3). Analogues were prepared with prenyl, geranyl and farnesyl side chains (22–24), as well as varying saturated/unsaturated motifs (25–27 and 11). Notably, while all of these analogues retained the substituted γ -pyrone of lehualide B, none of them showed significant antimyeloma activity (all had EC_{50} values $>1 \mu\text{M}$ in U266 MM cells; Figure 5B), indicating a significant role for the stereodefined skipped polyene subunit of the natural product.

Series II analogues assessed the effect of alterations to the tail of the hydrophobic linker (Figure 5C) while maintaining the functionalized 2,3-dimethoxy-5,6-dimethyl- γ -pyrone core and the hydrophobic polyunsaturated linker. Analogues were prepared from the general sequence shown in Figure 5C, defined by Grignard addition to an unsaturated pyrone-containing aldehyde, followed by Ti-mediated alkoxide-directed reductive cross-coupling. While derivatives 28–30 showed substantially diminished anti-MM activity (EC_{50} 's of 100–600 nM), a variety of other substitutions were tolerated in this region. The most active analogues prepared include the C15- and C16-biphenyls (31 and 35; EC_{50} 's of 10–12 nM) and the C12-Et substituted variant 36 ($EC_{50} = 13$ nM) (Figure 5D). Other analogues possessing notable activity include the C14-Ph (32; EC_{50} 60 nM), the C-15 protio (33; EC_{50} 30 nM), the C15-TMS (21; EC_{50} 20 nM) and the C15 chloropentyl derivative (34; EC_{50} 60 nM).

Finally, Series III analogues were synthesized to determine the effects of subtle structural perturbations about the pyrone headgroup (Figure 6A). The synthesis of each analogue within this series was accomplished in a fashion akin to that described for lehualide B synthesis (Scheme 1D), where the variation in structure of the pyrone was introduced at the beginning of each sequence.

As illustrated, deletion of the 2,3-dimethoxy substituent of lehualide B essentially abolished antimyeloma activity, where compounds 37 and 38 displayed markedly reduced abilities to inhibit the growth of U266 MM cells ($EC_{50} > 1 \mu\text{M}$). Notably, substitution α - to the pyrone also obliterated the cytotoxic properties of lehualide B. For example, analogue 41 that houses a prenyl substituent at this position did not inhibit MM or lymphoma cell growth at concentrations greater than $1 \mu\text{M}$. The most potent Series III analogues were those that simply replaced the C3 methyl ether of the pyrone with an ethyl group. Analogues 42–44 were the most active members of this series, with EC_{50} values vs U266 MM cells of 19, 3, and 20 nM, respectively.

Antimyeloma Effects of Lehualide B Analogues. The effects of lehualide B and top analogues showing antimyeloma and lymphoma activity in MTT assays suggested that they would also compromise the long-term, anchorage-independent growth of MM in methylcellulose colony assays.⁴⁶ Indeed, treatment with lehualide B, 36, 42, or 43 completely abolished colony formation of NCI H929 and U266 MM cells (Figure 6B–D), further supporting their potential use as antimyeloma agents.

Over 70 000 patients in the United States currently suffer from multiple myeloma (MM), with 20 000 new cases and 10

000 deaths per year.⁴⁷ Morbidity associated with this malignancy is very high, with patients experiencing anemia, chronic bone pain and fractures, and an overall 5-year survival still below 40% despite aggressive chemotherapy, up-front bone marrow transplantation, the novel use of agents such as thalidomide, and the development of new drugs such as bortezomib.

The marine-derived natural product lehualide B was originally reported to have modest activity against IGROV-ET ovarian cancer cells.⁴ While no other biological properties had been assigned to this compound, its modest activity, unique chemical structure, and lack of availability from natural sources stimulated our interest in exploring a means to prepare this compound (and related derivatives) in the laboratory to fuel efforts focused on thoroughly evaluating its efficacy as an anticancer agent.

Notably, we achieved a concise synthesis of this target in just eight steps from a simple γ -pyrone through a sequence that highlights the unique and divergent stereochemical course of allylic alcohol–alkyne reductive cross-coupling when compared to the Claisen rearrangement. Both processes were used back-to-back to establish the entire stereodefined hydrophobic tail of lehualide B and generated each of the three trisubstituted alkenes with just four carbon–carbon bond forming reactions (Claisen rearrangement, Grignard addition, Ti-mediated reductive cross-coupling and Negishi coupling).

The concise nature of this synthesis fueled our pursuits that have defined the substantial anti-multiple myeloma properties of lehualide B. In short order it was discovered that lehualide B possesses rather profound and selective anti-multiple myeloma activity, having low nanomolar EC_{50} activity in human MM and Raji B lymphoma and low or no activity against human breast cancer.

Our studies established that lehualide B has similar activity to piericidin A1 as a potent inhibitor of complex I. Establishing this relationship led to the discovery that piericidin A1 also has selective activity against MM. These findings add to the interesting anticancer profile of piericidin A1 that, to date, includes toxicity against human NSCLC, leukemia and colon carcinoma.^{28,48–50} We conclude that at least some mitochondrial complex I inhibitors, specifically lehualide B and piericidin A1, are selective anticancer agents that have profound cytotoxic activity against chemoresistant multiple myeloma cells. Further, our studies suggest that tumor types that rely on OXPHOS to support their metabolism, such as MM, will be exquisitely sensitive to complex I inhibitors such as lehualide B. Finally, the sensitivity of MM cells to complex I inhibitors may also reflect the massive production of immunoglobulins and inherently high activity of the endoplasmic reticulum (ER) in this tumor type.⁵¹ Specifically, mitochondria function to balance Ca^{2+} pools in the lumen of ER, and their inhibition would lead to Ca^{2+} loss and cell death.

Our *in vivo* evaluations of lehualide B revealed that dosing *i.p.* (1 mg/kg) in sub-Q transplant models of RPMI 8226 and U266 MM cells led to tumor drug concentrations that were an order of magnitude higher than the EC_{50} value of lehualide B in cellular assays. While promising, much higher concentrations were, however, found in fat, kidney and heart. The relevance of tissue distribution data are difficult to extrapolate across species, yet these findings indicate that the DMPK profile for lehualide B (and perhaps its analogues) needs substantial improvement or that a targeted drug delivery strategy needs to be established before advancing as a clinically relevant antimyeloma agent.

The compelling anti-multiple myeloma profile of lehualide B prompted the investigation of structure–activity relationships associated with the natural product. Over 20 analogues were prepared to evaluate the role of three regions of the natural product skeleton (the hydrophobic tail terminus, the hydrophobic polyunsaturated linker, and the hydrophilic headgroup) in anticancer activity. These studies led to the general summary of SAR illustrated in Figure 7 and include the following

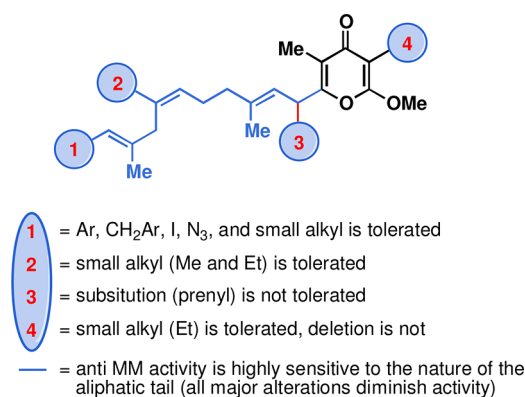


Figure 7. Summary of lehualide B analogues: SAR for anti-MM activity.

features: (1) The stereodefined skipped-polyunsaturated hydrophobic tail plays a critical role in cytotoxicity. This observation is similar to that observed with piericidin analogues, where simplified hydrophobic chains appended to the pyridine core compromise cytotoxicity.²⁸ Similar trends have also been observed with verticypyrone.⁵² (2) The terminal substituents of the hydrophobic chain of lehualide B play an important role in anti-MM activity. Small substituents are optimal at C15, while some modifications of C16 functionality are tolerated (small alkyl and aryl). (3) Anti-MM activity is sensitive to the substitution of the pyrone headgroup. The only synthetic analogues that possess similar activity to the natural product had a simple change of substitution at C3 of the pyrone from OMe to Et. All other attempted modifications to this region of the natural product markedly reduced anti-MM activity.

Overall, these studies have established a chemical foundation suitable for the production of lehualide-inspired agents. This achievement led to the elucidation of lehualide B's activity as a complex I inhibitor and the discovery that this natural product possesses profound anti-multiple myeloma properties. While the development of lehualide B as a chemotherapeutic agent is anticipated to be challenging, the chemical advance central to these studies provides a means to drive the search for therapeutically relevant natural product analogues.

■ ASSOCIATED CONTENT

Supporting Information

Experimental procedures and tabulated spectroscopic data for new compounds. This material is available free of charge via the Internet at <http://pubs.acs.org>.

■ AUTHOR INFORMATION

Corresponding Author

*E-mail: micalizio@scripps.edu; jcleve@scripps.edu.

Notes

The authors declare no competing financial interest.

■ ACKNOWLEDGMENTS

We gratefully acknowledge financial support of this work by grants from the National Institutes of Health/NIGMS (GM80266, GM80266-04S1, to G.C.M.) and NCI (CA076379, to J.L.C.), and by monies from the State of Florida to Scripps Florida.

■ REFERENCES

- (1) Morris, E. (2006) Marine natural products: Drugs from the deep. *Nature* 443, 904–905.
- (2) Miller, J. H., Singh, A. J., and Northcote, P. T. (2000) Microtubule-stabilizing drugs from marine sponges: focus on peloruside A and zampanolide. *Marine Drugs* 8, 1059–1079.
- (3) Simmons, T. L., Andrianasolo, E., McPhail, K., Flatt, P., and Gerwick, W. H. (2005) Marine natural products as anticancer drugs. *Mol. Cancer Ther.* 4, 333–342.
- (4) Sata, N., Abinsay, H., Yoshida, W. Y., Horgen, F. D., Sitachitta, N., Kelly, M., and Scheuer, P. J. (2005) Lehualides A–D, metabolites from a Hawaiian sponge of the genus *Plakortis*. *J. Nat. Prod.* 68, 1400–1403.
- (5) Barber, J. M., Quek, N. C. H., Leahy, D. C., Miller, J. H., Bellows, D. S., and Northcote, P. T. (2011) Lehualides E–K, cytotoxic metabolites from the Tongan marine sponge *Plakortis* sp. *J. Nat. Prod.* 74, 809–815.
- (6) Wilk, W., Waldmann, H., and Kaiser, M. (2009) Gamma-pyrone natural products—a privileged compound class provided by nature. *Bioorg. Med. Chem.* 17, 2304–2309.
- (7) Wetzel, S., Wilk, W., Chammaa, S., Sperl, B., Roth, A. G., Yektaoglu, A., Renner, S., Berg, T., Arenz, C., Giannis, A., Oprea, T. I., Rauh, D., Kaiser, M., and Waldmann, H. (2010) A scaffold-tree-merging strategy for prospective bioactivity annotation of gamma-pyrones. *Angew. Chem., Int. Ed.* 49, 3666–3670.
- (8) Foucher, B., Chappell, J. B., and McGivan, J. D. (1974) The effects of acetylcolletotrichin on the mitochondrial respiratory chain. *Biochem. J.* 138, 415–423.
- (9) Singh, S. B., Zink, D. L., Dombrowski, A. W., Dezeny, G., Bills, G. F., Felix, J. P., Slaughter, R. S., and Goetz, M. A. (2001) Candelalides A–C: Novel diterpenoid pyrones from fermentations of *Sesquicillium candelabrum* as blockers of the voltage-gated potassium channel Kv1.3. *Org. Lett.* 3, 247–250.
- (10) Goetz, M. A., Zink, D. L., Dezeny, G., Dombrowski, A., Polishook, J. D., Felix, J. P., Slaughter, R. S., and Singh, S. B. (2001) Diterpenoid pyrones, novel blockers of the voltage-gated potassium channel Kv1.3 from fungal fermentations. *Tetrahedron Lett.* 42, 1255–1257.
- (11) Bills, G. F., Polishook, J. D., Goetz, M. A., Sullivan, R. F., and White, J. F., Jr. (2002) *Chaunopycnis pustulata* sp. nov., a new clavicipitalean anamorph producing metabolites that modulate potassium ion channels. *Mycol. Prog.* 1, 3–17.
- (12) Gupta, S., Krasnoff, S. B., Renwick, J. A. A., Roberts, D. W., Steiner, J. R., and Clardy, J. (1993) Viridoxins A and B: novel toxins from the fungus *Metarhizium flavoviride*. *J. Org. Chem.* 58, 1062–1067.
- (13) Ui, H., Shiomi, K., Suzuki, H., Hatano, H., Morimoto, H., Yamaguchi, Y., Masuma, R., Sunazuka, T., Shimamura, H., Sakamoto, K., Kita, K., Miyoshi, H., Tomoda, H., and Omura, S. (2006) Verticypyrone, a new NADH-fumarate reductase inhibitor, produced by *Verticillium* sp. FKI-1083. *J. Antibiot.* 59, 785–790.
- (14) Kurosawa, K., Takahashi, K., Fujise, N., Yamashita, Y., Washida, N., and Tsuda, E. (2002) SNF4435C and D, novel immunosuppressants produced by a strain of *Streptomyces spectabilis*. III. Immunosuppressive efficacy. *J. Antibiot.* 55, 71–77.
- (15) Ueda, J., Hashimoto, J., Nagai, A., Nakashima, T., Komaki, H., Anzai, K., Harayama, S., Doi, T., Takahashi, T., Nagasawa, K., Natsume, T., Takagi, M., and Shin-ya, K. (2007) New aureothin derivative, alloaureothin, from *Streptomyces* sp. MIM23. *J. Antibiot.* 60, 321–324.
- (16) Kurosawa, K., Takahashi, K., and Tsuda, E. (2001) SNF4435C and D, novel immunosuppressants produced by a strain of

Streptomyces spectabilis. I. Taxonomy, fermentation, isolation, and biological activities. *J. Antibiot.* 54, 541–547.

(17) Takahashi, K., Tsuda, E., and Kurosawa, K. (2001) SNF4435C and D, novel immunosuppressants produced by a strain of *Streptomyces spectabilis*—II. Structure elucidation. *J. Antibiot.* 54, 548–553.

(18) Yano, K., Yokoi, K., Sato, J., Oono, J., Kouda, T., Ogawa, Y., and Nakashima, T. (1986) Actinopyrones A, B and C, new physiologically active substances. II. Physico-chemical properties and chemical structures. *J. Antibiot.* 39, 38–43.

(19) Yano, K., Yokoi, K., Sato, J., Oono, J., Kouda, T., Ogawa, Y., and Nakashima, T. (1986) Actinopyrones A, B and C, new physiologically active substances. *J. Antibiot.* 39, 32–37.

(20) Taniguchi, M., Watanabe, M., Nagai, J., Suzumura, K.-I., Suzuki, K.-I., and Tanaka, A. (2000) γ -Pyrone compounds with selective and potent anti-*Helicobacter pylori* activity. *J. Antibiot.* 53, 844–847.

(21) Graber, M. A., and Gerwick, W. H. (1998) Kalkipyron, a toxic γ -pyrone from an assemblage of the marine cyanobacteria *Lyngbya majuscula* and *Tolypothrix* sp. *J. Nat. Prod.* 61, 677–680.

(22) Yoshida, S., Yoneyama, K., Shiraishi, S., Watanabe, A., and Takahashi, N. (1977) Isolation and physical properties of new piericidins produced by *Streptomyces pactum*. *Agric. Biol. Chem.* 41, 849–853.

(23) Yoshida, S., Yoneyama, K., Shiraishi, S., Watanabe, A., and Takahashi, N. (1977) Chemical structures of new piericidins produced by *Streptomyces pactum*. *Agric. Biol. Chem.* 41, 855–862.

(24) Kimura, K., Takahashi, H., Miyata, N., Yoshihama, M., and Uramoto, M. (1996) New piericidin antibiotics, 7-demethylpiericidin A1 and 7-demethyl-3'-rhamnopericidin A1. *J. Antibiot.* 49, 697–699.

(25) For the combinatorial synthesis and evaluation of a collection of benzopyran natural product-like inhibitors of NADH:ubiquinone oxidoreductase, see: Nicolaou, K. C., Pfefferkorn, J. A., Schuler, F., Roecker, A. J., Cao, G.-Q., and Casida, J. E. (2000) Combinatorial synthesis of novel and potent inhibitors of NADH:ubiquinone oxidoreductase. *Chem. Biol.* 7, 979–992.

(26) Shimamura, H., Sunazuka, T., Izuhara, T., Hirose, T., Shiomi, K., and Omura, S. (2007) Total synthesis and biological evaluation of verticypyrone and analogues. *Org. Lett.* 9, 65–67.

(27) Udeani, G. O., Geräuser, C., Thomas, C. F., Moon, R. C., Kosmeder, J. W., Kinghorn, A. D., Moriarty, R. M., and Pezzuto, J. M. (1997) Cancer chemopreventive activity mediated by deguelin, a naturally occurring rotenoid. *Cancer Res.* 57, 3424–3428 and references therein.

(28) Schnermann, M. J., Romero, F. A., Hwang, I., Nakamaru-Ogiso, E., Yagi, T., and Boger, D. L. (2006) Total synthesis of piericidin A1 and B1 and key analogues. *J. Am. Chem. Soc.* 128, 11799–11807.

(29) Jeso, V., and Micalizio, G. C. (2010) Total synthesis of lehualide B by allylic alcohol–alkyne reductive cross-coupling. *J. Am. Chem. Soc.* 132, 11422–11424.

(30) For a recent example that highlights the sensitivity of β,γ -unsaturated carbonyls, see: Gagnepain, J., Moulin, E., and Fürstner, A. (2011) Gram-scale synthesis of leijimalide B. *Chem.—Eur. J.* 17, 6964–6972.

(31) For a review of palladium-catalyzed cross-coupling reactions in total synthesis, see: Nicolaou, K. C., Bulger, P. G., and Sarlah, D. (2005) Palladium-catalyzed cross-coupling reactions in total synthesis. *Angew. Chem., Int. Ed.* 44, 4442–4489.

(32) Kolundzic, F., and Micalizio, G. C. (2007) Synthesis of substituted 1,4-dienes by direct alkylation of allylic alcohols. *J. Am. Chem. Soc.* 129, 15112–15113.

(33) Rhoads, S. J., and Raulins, R. (1975) Claisen and Cope rearrangements. *Org. React.* 22, 1–74.

(34) Ziegler, F. E. (1988) The thermal, aliphatic Claisen rearrangement. *Chem. Rev.* 88, 1423–1452.

(35) The procedure employed is a variation of that reported: Moriarty, R. M., Vaid, R. K., Ravikumar, V. T., Vaid, B. K., and Hopkins, T. E. (1988) Hypervalent iodine oxidation: α -functionalization of β -dicarbonyl compounds using iodosobenzene. *Tetrahedron* 44, 1603–1607.

(36) For an early example of pyrone formation conducted in sulfuric acid (conc.), see: Light, R. J., and Hauser, C. R. (1960) Aroylations of β -diketones at the terminal methyl group to form 1,3,5-triketones. *J. Org. Chem.* 25, 538–546.

(37) Jones, D. N., Mundy, D., and Whitehouse, R. D. (1970) Steroidal selenoxides diastereoisomeric at selenium; *syn*-elimination, absolute configuration, and optical rotatory dispersion characteristics. *Chem. Commun.*, 86–87.

(38) For an early example, see: Johnson, W. S., Werthem, A. L., Bartlett, W. R., Brocksom, T. J., Li, T. T., Faulkner, D. J., and Petersen, M. R. (1970) Simple stereoselective version of the Claisen rearrangement leading to *trans*-trisubstituted olefinic bonds. Synthesis of squalene. *J. Am. Chem. Soc.* 92, 741–743.

(39) Reichard, H. A., McLaughlin, M., Chen, M. Z., and Micalizio, G. C. (2010) Regioselective reductive cross-coupling reactions of unsymmetrical alkynes. *Eur. J. Org. Chem.*, 391–409.

(40) Anderson, J. E. (1974) Conformational analysis of cyclohexane derivatives. The A value of a benzyl group. *J. Chem. Soc., Perkin Trans.* 2, 10–13.

(41) Stamos, D. P., Taylor, A. G., and Kishi, Y. (1996) A mild preparation of vinyl iodides from vinylsilanes. *Tetrahedron Lett.* 37, 8647–8650.

(42) For a recent review, see: Jana, R., Pathak, T. P., and Sigman, M. S. (2011) Advances in transition metal (Pd, Ni, Fe)-catalyzed cross-coupling reactions using alkyl-organometallics as reaction partners. *Chem. Rev.* 111, 1417–1492.

(43) The MTT assay is a colorimetric assay for measuring the activity of enzymes that reduce 3-(4,5-dimethylthiazol-2-yl)-2,5-diphenyltetrazolium bromide (MTT). This reduction takes place only when reductase enzymes are active, and therefore conversion is often used as a measure of viable (living) cells. See: Mosmann, T. (1983) Rapid colorimetric assay for cellular growth and survival: application to proliferation and cytotoxicity assays. *J. Immunol. Methods* 65, 55–63.

(44) The dye exclusion test is used to determine the number of viable cells present in a cell suspension. It is based on the principle that live cells possess intact cell membranes that exclude certain dyes, such as trypan blue, Eosin, or propidium, whereas dead cells do not. Overall, dye exclusion is a simple and rapid technique to measure cell viability indirectly via assessment of cell membrane integrity. See: Strober, W. (1997) Trypan blue test of cell viability. *Curr. Protoc. Immunol.* A.3B.1–A.3B.2.

(45) Wu, M., Neilson, A., Swift, A. L., Moran, R., Tamagnine, J., Parslow, D., Armistead, S., Lemire, K., Orrell, J., Teich, J., Chomicz, S., and Ferrick, D. A. (2007) Multiparameter metabolic analysis reveals a close link between attenuated mitochondrial bioenergetic function and enhanced glycolysis dependency in human tumor cells. *Am. J. Physiol.: Cell Physiol.* 292, C125–136.

(46) Li, Y., Li, Ching, J., Yu, D., and Pardee, A. B. (2000) Potent induction of apoptosis by beta-lapachone in human multiple myeloma cell lines and patient cells. *Mol. Med.* 6, 1008–1015. MTT assays assess the short-term anti-proliferative effects of anticancer agents, while methylcellulose colony assays are a more rigorous measure of the effects of such agents on long-term, anchorage-independent growth of tumor cells in semi-solid medium.

(47) Mahindra, A., Laubach, J., Raje, N., Munshi, N., Richardson, P. G., and Anderson, K. (2012) Latest advances and current challenges in the treatment of multiple myeloma. *Nat. Rev. Clin. Oncol.* 9, 135–143.

(48) Urakwa, A., Sasaki, T., Yoshida, K., Otani, T., Lei, Y., and Yun, W. (1996) IT-143-A and B, novel piericidin-group antibiotics produced by *Streptomyces* sp. *J. Antibiot.* 49, 1052–1055.

(49) Hwang, J., Kim, J., Cha, M., Ryoo, I., Choo, S., Cho, S., Tsukumo, Y., Tomida, A., Shin, K., Hwang, Y., Yoo, I., and Park, H. (2008) Etoposide-resistant HT-29 human colon carcinoma cells during glucose deprivation are sensitive to piericidin A, a GRP78 down-regulator. *J. Cell. Physiol.* 215, 243–250.

(50) Kitaura, N., Shirata, K., Niwano, M., Mimura, M., and Takahara, Y. (1993) Tumor cell inhibitors containing piericidin A, Japanese Patent 05339156 A2, *Chem. Abstr.* 1994, 120, 208590.

(51) Kurtoglu, M., Philips, K., Liu, H., Boise, L. H., and Lampidis, T. J. (2010) High endoplasmic reticulum activity renders multiple myeloma cells hypersensitive to mitochondrial inhibitors. *Cancer Chemother. Pharmacol.* 66, 129–140.

(52) Leiris, S. J., Khmour, O. M., Segerman, Z. J., Tsosie, K. S., Chapuis, J.-C., and Hecht, S. M. (2010) Synthesis and evaluation of verticipyrene analogues as mitochondrial complex I inhibitors. *Bioorg. Med. Chem.* 18, 3481–3493.